

# Design and Interpretation of Colliding Pulse Injected Laser-Plasma Acceleration Experiments

Estelle Cormier-Michel<sup>\*</sup>, Vahid H. Ranjbar<sup>\*</sup>, David L. Bruhwiler<sup>\*</sup>, Min Chen<sup>†</sup>, Cameron G. R. Geddes<sup>†</sup>, Eric Esarey<sup>†</sup>, Carl B. Schroeder<sup>†</sup> and Wim P. Leemans<sup>†</sup>

<sup>\*</sup>*Tech-X Corporation, 5621 Arapahoe Ave, Suite A, Boulder, CO 80303, USA*

<sup>†</sup>*LOASIS program, Lawrence Berkeley National Laboratory, 1 cyclotron road, Berkeley, CA 94720, USA*

**Abstract.** The use of colliding laser pulses to control the injection of plasma electrons into the plasma wake of a laser-plasma accelerator is a promising approach to obtaining GeV scale electron bunches with reduced emittance and energy spread. Colliding Pulse Injection (CPI) experiments are being performed by groups around the world. We present recent particle-in-cell simulations, using the parallel VORPAL framework, of CPI for physical parameters relevant to ongoing experiments of the LOASIS program at LBNL. We perform parameter scans in order to optimize the quality of the bunch, and compare the results with experimental data. Effect of non-ideal gaussian pulses and laser self-focusing in the plasma channel on the trapped bunch are evaluated. For optimized parameters accessible in the experiment, a 20 pC electron beam can be accelerated to 300 MeV with percent level energy spread.

**Keywords:** Laser-plasma accelerator, injection, colliding pulse, particle-in-cell simulation

**PACS:** 52.38.Kd, 41.75.Jv, 52.65.Rr

## INTRODUCTION

Laser-Plasma Accelerators (LPAs) offer a promising technique towards compact particle accelerators [1]. Narrow energy spread beams have been produced with this technique up to the GeV level [2]. In these experiments, production of the electron beam relied on self-trapping of the background plasma electrons, which depends sensitively on the self evolution of the laser field [3, 4, 5]. Even though stable beams have been reported by using this technique, they are for a small range of laser and plasma parameters [2, 6]. Applications of LPAs, such as high energy particle colliders and production of light sources (from X-rays to  $\gamma$ -rays) call for more stable and tunable sources of electrons. That is why controlled injection in LPA has been a topic of intense interest in the last few years. In particular, injection via colliding laser pulses is a promising method in terms of reproducibility and tunability of the electron beam, with low energy spread and emittance [7, 8, 9, 10, 11]. Current colliding pulse injection (CPI) experiments are carried out with two laser pulses where one of the two pulses also act as the driver for the plasma wakefield. The overlap of the two laser pulses, with same polarization, produces a slow phase velocity beat wave in which electrons from the background plasma can be trapped. When the trapped orbits of the slow wave intercept with the trapped orbits of the plasma wakefield created by the drive pulse, electrons can be pushed into the correct phase of the wakefield to be further accelerated, creating a low energy spread bunch at dephasing [7, 12].

In this paper we report self-consistent simulations of electron beam injection via colliding laser pulses, and subsequent acceleration, with the parallel VORPAL framework [13], relevant to the CPI experiments at LBNL [14]. Simulations were conducted over a wide range of parameters for both laser pulses and plasma profile, allowing conditions for the production of the best quality electron beam to be determined. In addition, self-consistent simulations allow understanding of the physics of the injection process, which will help optimize injection results. In the following we will present parameter scans which have been used to guide the experiments at LBNL on the production of high quality electron beams using CPI. We will also explore effects of the laser evolution on particle trapping and undesirable effects which can appear in the experiment such as the presence of non-Gaussian modes in the laser pulse.

## PARAMETER SCANS AND COMPARISON WITH EXPERIMENT

Simulations were conducted on CPI into highly nonlinear wakes. The experiments simulated use the 10 TW Ti:Sapphire laser system of the LOASIS Laboratory at LBNL. A 0.6 J, laser pulse is used to drive the wake with

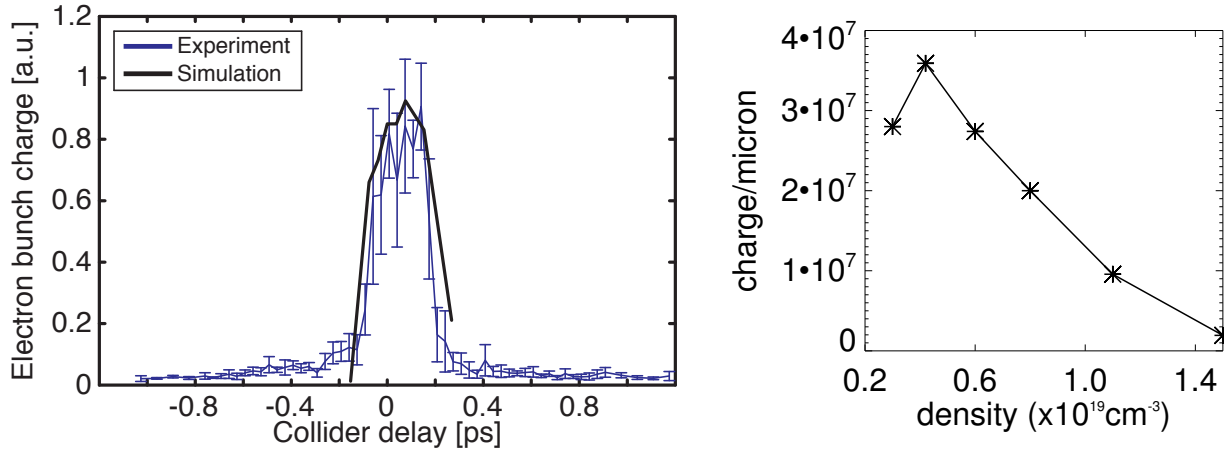


**FIGURE 1.** Amount of trapped charge as a function of (left) delay between the driver and collider pulses, (right) plasma density, for simulation and experiments.

a spot size of  $\sim 6 \mu\text{m}$  and a normalized intensity  $a_0 \sim 2$ , with  $a_0 \simeq 0.85 \times 10^{-9} \lambda [\mu\text{m}] (I [\text{W}\cdot\text{cm}^{-2}])^{1/2}$ , where  $\lambda$  is the laser wavelength and  $I$  is the laser intensity. A second laser pulse,  $< 0.25 \text{J}$ , 50 fs to 100 fs, with a spot size of  $\sim 10 \mu\text{m}$  and a normalized intensity of the order of 0.1 – 1 collides with the driver at a  $19^\circ$  angle in an hydrogen gas jet, with a density up to  $5 \times 10^{19} \text{cm}^{-3}$  [14]. In the following we refer to the laser parameters such that the normalized vector potential is of the form  $a = a_{0,1} \exp(-x^2/L_{0,1}^2) \exp(-r^2/w_{0,1})$ , with  $a_{0,1}$  the normalized peak amplitude,  $L_{0,1}$  the pulse length and  $w_{0,1}$  the laser spot size, the indices (0, 1) refer to the laser driver and the laser collider respectively.

Two-dimensional (2D) simulations are used to evaluate density, timing and collider intensity regimes for injection. Simulations show and experiment observe particle injection for collider intensity  $a_1 > 0.2$ , increasing with laser collider intensity and showing signs of saturation at  $a_1 \sim 1$ . As the charge increases the final electron beam energy decreases and the energy spread increases due to the effect of beam loading. Simulations confirm that, due to beam loading, the accelerating field variations inside the electron beam increases with charge, while field amplitude decreases, increasing the energy spread and decreasing the energy gain. A good compromise between charge, energy and energy spread lies around  $a_1 = 0.5$ , with  $a_0 = 2$  and a plasma density  $n_0 = 4.2 \times 10^{18} \text{cm}^{-3}$ . Delay scan between the driver and the collider pulses [Fig. 1 (left)] shows that the trapped charge stays almost constant, with a variation of about 20%, within a  $\pm 200 \text{fs}$  window, which correspond to  $\pm$  twice the collider laser length. This was verified by experimental results. The charge then drops rapidly outside this window. In further simulations, we choose to collide the two pulses at their center point. For the laser parameters described above, optimal trapped charge is found at a density of  $n_0 \simeq 4.2 \times 10^{18} \text{cm}^{-3}$ , as seen in Fig. 1 (right). This is consistent with experimental data, where injection due to colliding laser pulses is observed between  $2 \times 10^{18} \text{cm}^{-3}$  and  $5 \times 10^{18} \text{cm}^{-3}$  [14]. The presence of a density optimum can be explained as follow: (i) as laser parameters remain constant, the volume of the overlapping laser pulses stay the same, explaining the reduction of charge as the density decreases compare to the optimum density; (ii) at higher densities the laser driver length becomes long compared to the plasma wavelength, i.e., the resonant condition  $L_0 \sim \lambda_p$ , where  $\lambda_p = \sqrt{mc^2/4\pi n_0 e^2}$  is the plasma wavelength, is no longer satisfied and the laser pulse drives a lower intensity plasma wake, which increases the trapping threshold, leading to a reduction of the trapped charge. Indeed, the optimal trapped charge is observed for  $\lambda_p \simeq 16 \mu\text{m} \sim L_0$ .

## PREDICTION OF ACCELERATOR PERFORMANCE

Optimization of the injector and accelerator performances requires many simulations. Because three-dimensional (3D) simulations are too computationally expensive to perform thorough parameter scans, we compare 2D and 3D results to assure that 2D simulations can capture all the physics, hence allowing careful design of CPI experiments. 3D and 2D simulations were performed at the optimal density  $n_0 = 4.2 \times 10^{18} \text{cm}^{-3}$  with a channel depth matched

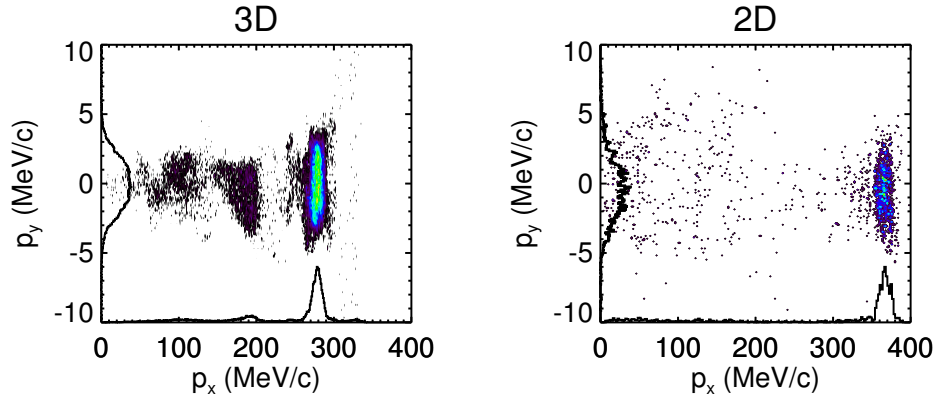


**FIGURE 2.** Longitudinal and transverse momentum of the trapped electron beam at dephasing for 3D (left) and 2D (right) simulations.

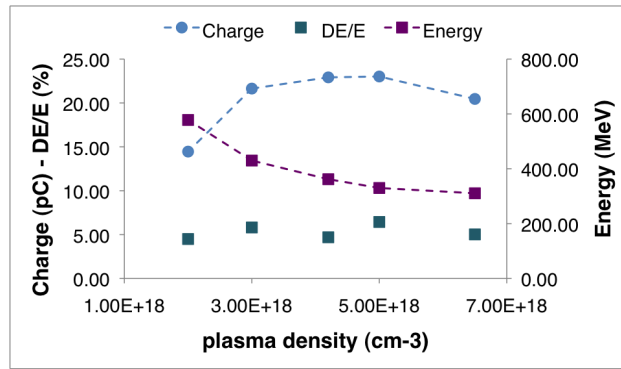


**FIGURE 3.** Density scan for laser driver parameters  $a_0 = 2$ ,  $w_0 = 6.14 \mu\text{m}$ ,  $L_0 = 9.7 \mu\text{m}$  and laser collider parameters  $a_1 = 0.5$ ,  $w_1 = 11 \mu\text{m}$  and  $L_1 = 18 \mu\text{m}$ . The channel depth is matched to a spot size  $w_M = 9.2 \mu\text{m}$ .

to a spot size  $w_M = 9.2 \mu\text{m}$ , a driver pulse intensity, spot size and length of  $a_0 = 2$ ,  $w_0 = 6.14 \mu\text{m}$ ,  $L_0 = 9.7 \mu\text{m}$  respectively, and a collider pulse intensity, spot size and length of  $a_1 = 0.5$ ,  $w_1 = 11 \mu\text{m}$  and  $L_1 = 18 \mu\text{m}$  respectively. Fig. 2 shows the trapped electron beam longitudinal and transverse momentum at dephasing for both 3D (left) and 2D (right) simulations. In both cases, the beam has a small energy spread ( $\simeq 2\%$  rms, if considering only the main peak), and a normalized emittance of the order of 2 mm mrad. The charge of the main beam in 3D is 20 pC. We observe that we can obtain a similar charge from the 2D simulation by multiplying the charge per unit length by the laser spot size. Hence, 2D simulations can represent the trapping and acceleration process accurately, albeit  $\simeq 30\%$  difference in the final energy, due to stronger loading of the wake in 3D.

2D parameter scans are then performed, with the plasma channel, to predict the behavior of the injector. Keeping the laser parameters constant, as in an experiment, while changing the plasma density can provide a way to tune the parameters of the bunch. This is shown in Fig. 3 where the plasma density is changed. We can see that the energy of the bunch increases with decreasing density due to the change in dephasing length. However, for densities between  $\simeq 3 \times 10^{18} \text{cm}^{-3}$  and  $\simeq 6 \times 10^{18} \text{cm}^{-3}$  all the other beam parameters (i.e., charge, energy spread, beam spot size and emittance) stay nearly constant. Note that, for consistency purposes, we represented here the rms energy spread, which stays around 5%, and whose calculations often include tails of the energy spectrum. However the full-width-half-maximum of the energy spectrum can reach values as low as 1%. Also, we can note that the density scale is different from the plot in Fig. 1, which scan is done without the plasma channel, hence the difference in behavior. However, we observe here again an optimum for the trapped charge around  $n_0 \simeq 4.2 \times 10^{18} \text{cm}^{-3}$ . On the other hand, scaling all laser parameters with the plasma density, i.e. the ratio of lengths over the plasma wavelength is kept constant, shows that the linear scaling laws also apply for the properties of the electron beam. One can then design an experiment, in terms of laser parameters and plasma density, depending on the beam properties required for applications.

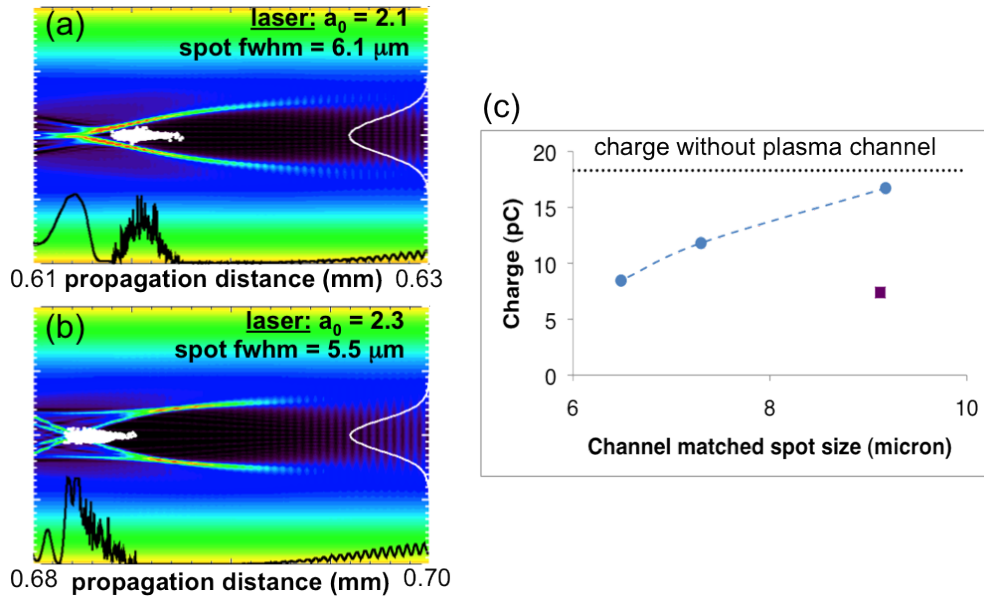


**FIGURE 4.** (a)-(b) Plasma density profile at different propagation distances with the trapped particles overlain in white. The curve on the right shows the laser transverse profile. (c) Amount of trapped charge as a function of channel matched radius; the blue circles indicate the laser being focused at the left of the box while the purple square is for the laser being focused at the interaction point.

## EFFECTS OF THE EVOLUTION OF THE PLASMA BUBBLE ON THE TRAPPED BUNCH

Introducing a plasma channel prevents the driver laser pulse from diffracting, keeping the accelerating field high over the whole acceleration length and allowing for higher energy gain of the trapped electron beam. As the power of the laser driver is close to the critical power, the channel depth needs to be relaxed from its matching condition, given by a transverse plasma profile of the form  $n(r) = n_0 + \Delta n_c (r/w_M)^2$ , with  $\Delta n_c [\text{cm}^{-3}] = 1.13 \times 10^{20} / w_M^2 [\mu\text{m}]$  and  $w_M$  the channel matched radius, to compensate for self-focusing.

We observe that if the laser pulse self-focuses some of the initial trapped charge is lost. This is due to the fact that the bubble gets shorter as the spot size of the laser pulse gets smaller. As the bubble length shrinks, the trapped charge located at the back of the bubble can end up in defocusing phase, leading to truncation of the bunch charge. This is represented in Fig. 4 (a)-(b), where the plasma density is shown with the trapped particles overlain in white. The transverse profile of the laser pulse is also represented on the right side of the plot. We can see that as the laser focuses, the bubble shortens, resulting in loss of charge which is defocused. Several channel matched radii were used, for a laser driver with initial intensity of  $a_0 = 2$ , spot size  $w_0 = 6.14 \mu\text{m}$ , and length  $L_0 = 9.7 \mu\text{m}$ , in a plasma density  $n_0 = 4.2 \times 10^{18} \text{cm}^{-3}$ , i.e.  $P/P_c \simeq 0.7$ , where  $P$  is the laser power and  $P_c$  is the critical power at this density. Fig. 4 (c) shows the final trapped charge as a function of the matched radius of the channel,  $w_M$ , when the laser is focused at the left of the plasma ramp (blue circles). As the depth of the channel gets closer to the matching condition, i.e.,  $w_M$  gets smaller, the laser pulse self-focuses sooner after the trapping occurs, leading to loss of more of the bunch charge. For a channel matched radius  $w_M = 9.2 \mu\text{m}$ , the final trapped charge is similar to the trapped charge without the plasma channel, however the final energy of the bunch is 2 times higher at dephasing, due to the fact that the laser pulse has not diffracted. The purple square on Fig. 4 (c) represent the final trapped charge, with a matched channel radius  $w_M = 9.2 \mu\text{m}$ , for the case where the laser pulse is focused at the point of the interaction, i.e. inside the plasma instead of at the entrance. Because the laser continue to focus during and after the interaction, less charge is trapped, showing the importance of controlling the focus point of the laser pulse, as well as the depth of the plasma channel.

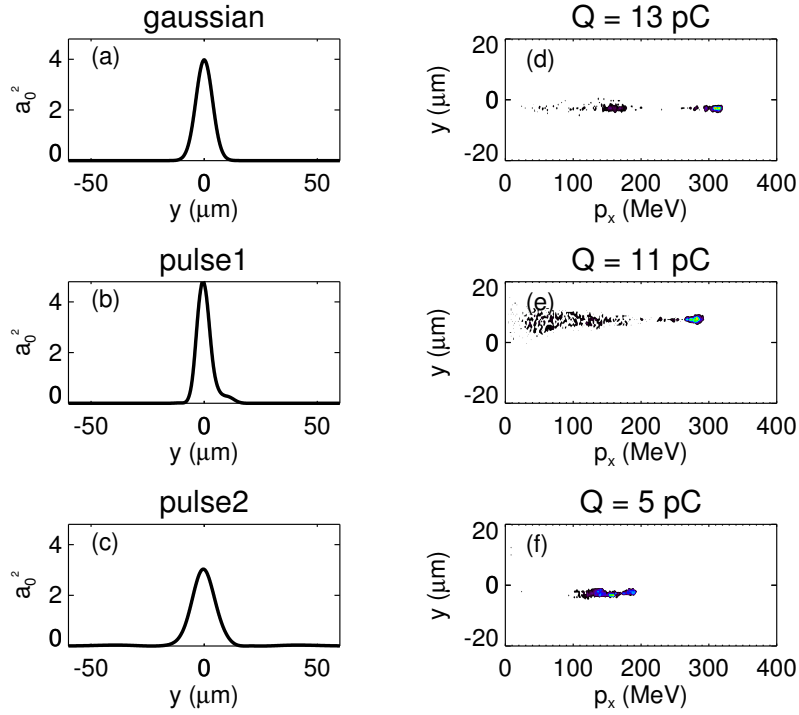


**FIGURE 5.** Transverse profile of (a) the ideal gaussian laser mode, and of laser pulses with Hermite-Gaussian modes up to third order: (b) *pulse1* and (c) *pulse2*, with (d)-(f) corresponding trapped electron beam transverse position ( $y$ ) as a function of longitudinal momentum ( $p_x$ ). The amount of trapped charge is also indicated.

## EFFECTS OF REALISTIC LASER MODES ON TRAPPING

High power lasers used to drive experiments have modes which are not perfectly gaussian. 2D simulations were used to evaluate the impact of such modes on quality of the trapped bunch. We fit laser profiles from experimental data with a sum of a fundamental gaussian pulse and higher order Hermite-Gaussian modes, up to third order. The simulated transverse profiles of the driver pulse, at the start of the simulation, are shown in Fig. 5 (a)-(c) with the corresponding electron beam profile at the end of the simulation, Fig. 5 (d)-(f). Fig. 5 (a) shows the perfect gaussian mode, as usually simulated, with  $a_0 = 2$  and  $w_0 = 7.26 \mu\text{m}$ . The length of the pulse is  $L_0 = 11.5 \mu\text{m}$ . The main gaussian component of the first pulse with higher order modes [*pulse1*, shown in Fig. 5 (b)] has higher intensity and smaller spot size ( $a_0 = 2.1$  and  $w_0 = 6.14 \mu\text{m}$ ), with an additional lobe at  $\simeq 11 \mu\text{m}$ . The second pulse with higher order modes [*pulse2*, shown in Fig. 5 (c)] has a lower intensity due to a larger spot size ( $a_0 = 1.7$  and  $w_0 = 9.37 \mu\text{m}$ ) in the main gaussian component and two additional lobes at  $y = \pm 42 \mu\text{m}$ . The collider pulse is a perfect gaussian mode with  $a_1 = 0.5$ ,  $w_1 = 11 \mu\text{m}$  and  $L_1 = 18 \mu\text{m}$ .

The trapped charge is principally dependent upon the product  $a_0 a_1$  [7, 12]. As a result, the amount of trapped charge for *pulse1*, is almost the same as for the ideal gaussian pulse. However, the presence of a lobe close to the main gaussian component causes the intensity profile to peak off axis as the mode evolves, resulting in a deviation of the trapped beam, as can be seen if Fig. 5 (e) where the beam is transversely displaced by  $\simeq 7 \mu\text{m}$  at dephasing. Because  $a_0$  has been reduced in *pulse2* and some of the pulse energy is lost in the side lobes, the amount of trapped charge is being reduced by 60% and the quality of the beam is degraded, as seen in Fig. 5 (f). Note that these simulations were performed without a plasma channel, resulting in diffraction of the modes as the pulse propagates. Presence of a plasma channel may cause the off-axis modes to oscillate [15] and further distort the wake. Note also that the charge is lower than observed in Fig. 4 (c) because we used a longer pulse in this case.

## CONCLUSION

Self-consistent, particle-in-cell simulations have been performed with the VORPAL framework to design colliding pulse injection experiments in the nonlinear wake regime. First experimental results show very good agreement with simulation data, which gives confidence in the ability of the simulations to predict experimental results. Simulations in both three- and two-dimensions show very good agreement on the final electron bunch properties, allowing us to perform parameter scans in 2D. We observe that, for fixed laser parameters, the energy of the beam can be tuned independently of the other beam parameters by simply changing the density. For density of the order of  $4 \times 10^{18} \text{ cm}^{-3}$ , 3D simulation shows a 20 pC beam accelerated to 300 MeV. The beam consistently has a few percent energy spread, which could be further improved by controlling the length of the electron bunch in order to control beam loading. Realistic effects such as presence of higher order laser modes in the driver pulse and self-focusing of the laser beam in a plasma channel have been evaluated, which can degrade significantly the quality of the bunch if not optimized. More control over the beam parameters can be obtained by using a three-pulse scheme where two collider pulses are used, independently of the laser driver, e.g., allowing separate control of beam charge and injection phase. This scheme will be used in upcoming simulations and experiments.

## ACKNOWLEDGMENTS

This work was supported by the Department of Energy, Office of National Nuclear Security Administration, NA-22, and Office of Science, Office of High Energy Physics under contract No. DE-AC02-05CH11231, and via the COMPASS SciDAC project, grant No. DE-FC02-07ER41499, and by Tech-X Corporation. This work used resources of the National Energy Research Scientific Computing Center, which is supported by the Office of Science of the U.S. Department of Energy under Contract No. DE-AC02-05CH11231.

## REFERENCES

1. E. Esarey, C. B. Schroeder, and W. P. Leemans, *Rev. Mod. Phys.* **81**, 1229–1285 (2009).
2. W. P. Leemans, B. Nagler, A. J. Gonsalves, C. Tóth, K. Nakamura, C. G. R. Geddes, E. Esarey, C. B. Schroeder, and S. M. Hooker, *Nature Phys.* **2**, 696–699 (2006).
3. S. P. D. Mangles, C. D. Murphy, Z. Najmudin, A. G. R. Thomas, J. L. Collier, A. E. Dangor, E. J. Divall, P. S. Foster, J. G. Gallacher, C. J. Hooker, D. A. Jaroszynski, A. J. Langley, W. B. Mori, P. A. Norreys, F. S. Tsung, R. Viskup, B. R. Walton, and K. Krushelnick, *Nature* **431**, 535–538 (2004).
4. C. G. R. Geddes, C. Toth, J. van Tilborg, E. Esarey, C. B. Schroeder, D. L. Bruhwiler, C. Nieter, J. Cary, and W. P. Leemans, *Nature* **431**, 538–541 (2004).
5. J. Faure, Y. Glinec, A. Pukhov, S. Kiselev, S. Gordienko, E. Lefebvre, J.-P. Rousseau, F. Burgy, and V. Malka, *Nature* **431**, 541–544 (2004).
6. J. Osterhoff, A. Popp, Z. Major, B. Marx, T. P. Rowlands-Rees, M. Fuchs, R. Hörlein, F. Grüner, D. Habs, F. Krausz, S. M. Hooker, and S. Karsch, “Stable Laser-Driven Electron Beams from a Steady-State-Flow Gas Cell,” in *Proceedings of the Thirteenth Advanced Accelerator Concepts Workshop*, edited by C. B. Schroeder, W. Leemans, and E. Esarey, AIP, 2009, vol. 1086, pp. 125–130.
7. E. Esarey, R. F. Hubbard, W. P. Leemans, A. Ting, and P. Sprangle, *Phys. Rev. Lett.* **79**, 2682–2685 (1997).
8. J. R. Cary, R. E. Giacone, C. Nieter, and D. L. Bruhwiler, *Phys. of Plasmas* **12**, 056704 (2005).
9. G. Fubiani, E. Esarey, C. B. Schroeder, and W. P. Leemans, *Phys. Rev. E* **73**, 026402 (2006).
10. J. Faure, C. Rechatin, A. Norlin, A. Lifschitz, Y. Glinec, and V. Malka, *Nature* **444**, 737–739 (2006).
11. C. Toth, E. Esarey, C. G. R. Geddes, W. P. Leemans, K. Nakamura, D. Panasenko, C. B. Schroeder, D. L. Bruhwiler, and J. R. Cary, “Colliding pulse injection experiments in non-collinear geometry for controlled laser plasma wakefield acceleration electrons,” in *Proceedings of PAC07, Albuquerque, NM, USA, 2007*.
12. C. B. Schroeder, P. B. Lee, J. S. Wurtele, E. Esarey, and W. P. Leemans, *Phys. Rev. E* **59**, 6037–6047 (1999).
13. C. Nieter, and J. R. Cary, *J. Comp. Phys.* **196**, 448–473 (2004).
14. G. R. Plateau, C. G. R. Geddes, N. H. Matlis, E. Cormier-Michel, D. Mittelberger, D. B. Thorn, K. Nakamura, E. Esarey, and W. P. Leemans, “Colliding Laser Pulses for Laser-Plasma Accelerator Injection Control,” in *these proceedings*, 2010.
15. A. J. Gonsalves, K. Nakamura, C. Lin, J. Osterhoff, S. Shiraishi, C. B. Schroeder, C. G. R. Geddes, C. Toth, E. Esarey, and W. P. Leemans, *Phys. of Plasmas* **17**, 056706 (2010).